Laboratory Investigation (2020) 100:824–836
https://doi.org/10.1038/s41374-020-0373-z

ARTICLE

TGFβ1-Smad canonical and -Erk noncanonical pathways participate in interleukin-17-induced epithelial–mesenchymal transition in Sjögren's syndrome

Margherita Sisto[1] · Loredana Lorusso[1] · Giuseppe Ingravallo[2] · Domenico Ribatti[1] · Sabrina Lisi[1]

Received: 5 November 2019 / Revised: 23 December 2019 / Accepted: 30 December 2019 / Published online: 10 January 2020

Abstract

Interleukin-17 (IL-17) is a pleiotropic cytokine that plays a primary role in triggering epithelial–mesenchymal transition (EMT) in many chronic inflammatory diseases. EMT plays a critical role in the progression of salivary gland (SG) fibrosis in primary Sjögren's syndrome (pSS). This study focused on the activation of the canonical TGF-β1/Smad2/3 and noncanonical TGF-β1/Erk1/2 pathways in IL-17-dependent TGFβ1-induced EMT in human SG epithelial cells (SGEC) derived from healthy subjects. The expression of phosphorylated Smad2/3 and Erk1/2 during IL-17 treatment-stimulated EMT was evaluated in healthy SGEC. Cotreatment with IL-17 and specific TGFβ receptor type I kinase inhibitor SB431542, or Erk 1/2 inhibitor U0126, abrogates the corresponding morphological changes and EMT phenotypic markers expression in healthy SGEC. Interestingly, inhibition of canonical TGFβ1/Smad2/3 signal transduction had no effect on activation of the noncanonical TGFβ1/Erk1/2/EMT pathway, suggesting that the two pathways act independently in activating IL-17-dependent EMT in SGEC.

Introduction

Fibrosis typically results from chronic inflammation, suggesting that although initially beneficial, the repair process becomes pathogenic when it escapes control, leading to pathological damage and ultimately to loss of organ function. Most chronic inflammatory disorders have in common the persistent release of a wide range of proinflammatory cytokines in the chronic inflammatory microenvironment, which dysregulate events, resulting in an excessive accumulation of fibrotic tissue at the site of injury and failure to restore tissue and physiological organ function [1–4].

Therefore, when tissue is damaged/wounded, a series of signaling events activate the immune system, leading to severe inflammatory responses that trigger epithelial–mesenchymal transition (EMT), a complex reprogramming process that gradually converts epithelial cells to mesenchymal-like cells [5], contributing to trigger pathological fibrosis [6–8]. The fibrotic process is the main pathological feature in many chronic autoimmune diseases, including rheumatoid arthritis, systemic lupus erythematosus, and primary Sjögren's syndrome (pSS) [9, 10]. pSS is a chronic autoimmune inflammatory disease primarily affecting exocrine glands, that leads to an impaired secretory function. The clinical picture predominantly features dry eyes and dry mouth [11, 12]. The persistent chronic inflammation is caused by a marked overexpression of proinflammatory cytokines thought to be involved in the pathological mechanisms underlying tissue fibrosis, particularly in the salivary tract [3, 13]. Previous studies have identified several chemokines, cytokines, and growth factors mediating EMT, such as TGF-β1, IL-17, and IL-22, which may trigger the development and progression of salivary gland (SG; SGs) fibrosis [14–16].

TGF-β1 is a multifunctional cytokine considered to be a potent profibrotic mediator and recognized to induce the fibrotic process [17]. A recent study demonstrated an aberrant upregulation of TGF-β1 in pSS SG, promoting morphological and functional mesenchymal changes in SG epithelial cells (SGEC) via activation of the TGF-β1/Smad/Snail signaling pathway [14]. TGF-β1 regulates EMT through two main pathways: the canonical Smad dependent pathway and a non-Smad signaling pathway [18]. Recent investigations

✉ Margherita Sisto
margherita.sisto@uniba.it

[1] Department of Basic Medical Sciences, Neurosciences and Sensory Organs (SMBNOS), Section of Human Anatomy and Histology, University of Bari "Aldo Moro", Bari, Italy

[2] Department of Emergency and Organ Transplantation (DETO), Pathology Section, University of Bari "Aldo Moro", Bari, Italy

have also demonstrated that the non-Smad pathway can mediate TGF-β1 fibrogenic responses, too [16, 18]. The Smad family is composed of various factors that are crucial for the activation of TGF-β1 signaling, but how they promote IL-17-induced EMT remains unclear. In addition, the TGF-β1 pathway may also signal through other Smad-independent signal transducers including Ras–extracellular signal-regulated kinase (Erk) [19]. Moreover, there is increasing evidence that the Erk signaling pathway is involved in chronic fibroproliferative conditions [16].

Since IL-17 has recently emerged as an attractive target for the treatment of autoimmune diseases [20] and there is also now evidence that IL-17 plays a primary role in the pathogenesis of pulmonary fibrosis [21] and SG fibrosis [16], in this study we speculate whether IL-17 may trigger Smad2/3 phosphorylation by upregulating TGFβ1 expression, and thereby contribute to SG fibrosis in pSS. Specific inhibitors of the canonical (SMAD signaling)- and noncanonical (Erk signaling)-TGF-β1-dependent pathways were therefore employed, allowing us to demonstrate that IL-17-dependent TGF-β1 release requires the participation of both the canonical and noncanonical signaling pathways to induce SG EMT-dependent fibrosis.

Materials and methods

Reagents used for cells treatment and antibodies

Recombinant human Interleukin-17 (IL-17) (50 ng/ml) was purchased from Sigma-Aldrich (St. Louis, MO). The following antibodies were used for the study: mouse anti-human TGF-β1 monoclonal antibody (mAb) (1:50, Santa Cruz Biotechnology, Santa Cruz, CA, USA), goat anti-human Smad2/3 polyclonal Ab (pAb) (1:100, R&D Systems, Minneapolis, MN, USA); goat anti-human p-Smad2/3 (Ser 423/425) pAb (1:100, Santa Cruz Biotechnology), mouse anti-human Erk1/Erk2 mAb or mouse anti-human phospho-Erk1/Erk2 mAb (both from R&D systems); mouse anti-human β-actin mAb clone AC-15 (1:100, Sigma-Aldrich, St. Louis, MO); mouse anti-human E-cadherin mAb (1:100, Dako, Santa Clara, CA, USA), mouse anti-human-vimentin mAb (1:100, Thermo Fisher Scientific, Waltham, MA, USA); TGF-β receptor type I kinase inhibitor SB-431542 (10 mM in DMSO) (R&D systems, Minneapolis, MN, USA); Erk inhibitor U0126 (Sigma-Aldrich) at 10 μM.

Patients and healthy subjects

The Department of Pathology, University of Bari Medical School, selected twenty pSS labial SGs biopsies (patients aged 64.5 ± 3.2 years) according to the 2016 pSS ACR/EULAR classification criteria [22]. These are based on the evaluation of five points: anti-SSA/Ro antibody positivity and focal lymphocytic sialadenitis with a focus score of ≥1 foci/4 mm^2, each scoring 3; an altered ocular staining score of ≥5 (or van Bijsterveld score of ≥4), a Schirmer's test data of ≥5 mm/5 min, and an unstimulated salivary flow rate of ≥0.1 ml/min, each scoring 1. Primary healthy SGEC cultures were set up from healthy volunteers (aged 62.8 ± 1.7 years, $N = 10$), affected by salivary mucoceles and employed in all experimental procedures. The healthy subjects did not complain of oral dryness, had no autoimmune disease and normal salivary function. Informed consent was obtained from all the subjects, and the study was approved by the local Ethics Committee.

Cell culture and treatment

Healthy subjects and pSS patients were subjected to the MSGs explant outgrowth technique from the lower lip [23]. The tissues were dissociated, by enzymatic and mechanical methods, into a suspension of single cells and plated on culture flasks. pSS dispersal cells were resuspended in McCoy's 5a modified medium supplemented with 10% heat-inactivated (56 °C for 30 min) FCS, 1% antibiotic solution, 2 mM L-glutamine, 50 ng ml^{-1} epidermal growth factor (EGF, Promega, Madison, WI, USA), 0.5 μg ml^{-1} insulin (Novo, Bagsvaerd, Denmark) and incubated at 37 °C, 5% CO_2 in air. Using 0.02% EDTA treatment, contaminating fibroblasts were removed, while immunocytochemical confirmation of the epithelial origin of cultured cells was routinely performed, as previously described [24]. The primary pSS SGEC cultures obtained were used as controls for TGF-β1 expression. Healthy human SGEC were grown in the same modified McCoy's 5A medium (Invitrogen) supplemented with 1% heat-inactivated FCS (to avoid excessive growth during treatment with TGF-β1). Healthy SGEC were stimulated with 50 ng/mL of IL-17 in the growth medium for 24–72 h and then harvested for future analyses. To inhibit TGF-β1-dependent EMT, SB-431542 (R&D systems, Minneapolis, MN, USA) was dissolved at a concentration of 10 mM in DMSO. IL-17-treated healthy human SGEC were incubated in medium supplemented with 10 mM of SB431542 [25] at 37 °C in a 5% CO_2 atmosphere. To inhibit Erk1/2 activation, U0126 (Sigma-Aldrich) [26] was dissolved at a concentration of 10 μM in DMSO and added to IL-17 treated healthy SGEC culture medium at 37 °C in a 5% CO_2 atmosphere for 24–72 h. All experiments were performed in triplicate and repeated three times.

Assessment of morphological EMT-related changes in SGEC

To confirm that IL-17 treatment determines the activation of TGF-β1/Smad1/2/Erk1/2-dependent EMT in healthy

SGEC, in vitro analysis of the morphological changes indicative of the EMT was performed on 72 h-treated SGEC with IL-17 (50 ng/mL), in the presence and the absence of the TGF-β receptor type I kinase inhibitor SB431542 (10 mM) and Erk1/2 inhibitor U0126 (10 μM). Changes in cell morphology were assessed under phase contrast light microscopy.

Amplification of gene transcripts by reverse transcriptase polymerase chain reaction (RT-PCR) and quantitative real-time PCR (q-RT PCR)

Total RNA from untreated healthy SGEC, pSS SGEC, IL-17-24h-treated healthy, and healthy SGEC treated with IL-17 + SB431542/U0126 for 24 h was isolated using the TRIzol reagent (Invitrogen, Carlsbad, CA, USA.). First-strand cDNA was synthesized by M-MLV reverse transcriptase (Promega, Madison, WI, USA) with 1 μg each of DNA-free total RNA sample and oligo-(dT)15 (Life Technologies, Grand Island, NY, USA). Equal amounts of cDNA were subsequently amplified by PCR in a 20 μl reaction mixture containing 2 μM of each sense and antisense primer, PCR buffer, 2.4 mM MgCl2, 0.2 mM each dNTP, 10 μl of transcribed cDNA, and 0.04 U/μlTaq DNA polymerase. The primers used to amplify cDNA fragments were as follows: TGF-β1, forward 5′-CC CAGCATCTGCAAAGCTC-3′ and reverse 5′-GTCAATG TACAGCTGCCGCA-3′; Smad2, forward 5′-ACTAACTT CCCAGCAGGAAT-3′ and reverse 5′-GTTGGTCACTTGT TTCTCCA-3′; Smad3, forward 5′-ACCAAGTGCATTAC CATCC-3′ and reverse 5′-CAGTAGATAACGTGAGGG AGCCC-3′; Erk1, forward, 5′-CCCCTGCGACCCCTTAA GATTTGTGATT-3′ and reverse, 5′-CAGGGAAGATGG GCCCCGGTTAGAGA-3′; Erk2, forward, 5′-GCGCGGGC CCCCCCCCGGAGATGGTC-3′ and reverse, 5′-TGAAG CGCAGTAAGATTTTT-3′; E-cadherin, forward 5′-TTCC CTGCGTATACCCTGGT-3′ and reverse 5′- GCGAAGA TACCGGGGGACACTCATGAG-3′; vimentin, forward 5′-AGGAAATGGCTCGTCACCTTCGTGAATA-3′ and reverse 5′-GGAGTGTCGGTTGTTAAGAACTAGAGCT-3′. The PCR cycling profile consisted of an initial denaturation step at 95 °C for 15 min, followed by 35 cycles of 94 °C for 60 s; 55 °C for 60 s; and 72 °C for 60 s. Then, the products of amplification were electrophoresed on 1.5% agarose gel containing ethidium bromide and visualized under ultraviolet transillumination. For qRT-PCR, forward and reverse primers for all the genes tested and the internal control gene β-2 microglobulin (part no. 4326319E; β2M) were from Applied Biosystems (Assays-On-Demand, Applied Biosystems). Each qPCR reaction was run in triplicate on an ABI PRISM 7700 sequence detector (Applied Biosystems). Relative gene mRNA expression ratios were calculated using the ΔΔCt formula, where Ct is the threshold cycle time value. The different expression of mRNA was deducted from $2^{-\Delta\Delta Ct}$

Data evaluation and sequence analysis

mRNA quantification data, based on the mean of a set of three independent experiments, were obtained with gel image software (Bio-Profil Bio-1D; ltf Labortechnik GmbH, Wasserburg, Germany), determining the intensity values for each band relative to GAPDH as reference, expressed as arbitrary units. The identity of each PCR product was confirmed by the size, and the purified products were directly sequenced using gene-specific forward or reverse primers.

Enzyme-linked immunosorbent assay (ELISA)

The concentration of TGF-β1 in untreated healthy and pSS SGEC, IL-17-48h-treated healthy, and healthy SGEC treated with IL-17 + SB-431542/U0126 for 48 h, was detected by ELISA using kits from Invitrogen (Carlsbad, CA, USA) according to the manufacturer's instructions.

Western blot analysis

Total cell lysates from untreated healthy and pSS SGEC, IL-17-48 h-treated healthy, and healthy SGEC treated with IL-17 + SB-431542/U0126 for 48 h were prepared using a buffer (200 μl) containing 1% Triton X-100, 50 mM Tris-HCl (pH 7.4), 1 mM PMSF, 10 μg/ml soybean trypsin inhibitor, and 1 mg/ml leupeptin. The homogenates were centrifuged at 10,000 × *g* for 10 min at 4 °C and Bradford's protein assay was used to determine the protein concentrations. The samples, in equal amounts, were resolved by electrophoresis on 10% SDS-polyacrylamide gels, transferred to nitrocellulose membranes and blotted under the following conditions: 200 mA (constant amperage), 200 V for 110 min. Blots were blocked by phosphate-buffered saline (PBS) pH 7.2 with 0.1 % (v/v) Tween 20, 5 % w/v nonfat dried milk for 1 h and washed three times with 0.1 % (v/v) Tween 20-PBS 1× (T-PBS). Then, the membranes were probed with the specific primary antibodies as reported above. The signals were developed with the chemoluminescence luminal reagent (Santa Cruz Biotechnology) according to the protocol procedure. After incubation with a stripping buffer (Thermo Scientific, Middletown, VA, USA), immunoblots were probed with mouse anti-human β-actin mAb clone AC-15 (1:100, Sigma-Aldrich, St. Louis, MO; 0.25 μg/ml) used as protein loading control.

Flow cytometry

Untreated healthy and pSS SGEC, IL-17-48h-treated healthy, and healthy SGEC treated with IL-17 + SB-431542/U0126 for 48 h were incubated with mouse anti-human TGF-β1 mAb, goat anti-human Smad2/3 pAb, goat anti-human phospho-Smad2/3 (Ser 423/425) pAb, mouse anti-

human phospho-Erk1/Erk2 mAb, mouse anti-human E-cadherin mAb, mouse anti-human-vimentin mAb as primary antibodies, and with secondary antibodies conjugated with Alexa fluor 488 (Invitrogen). Protein expression was analyzed with a Becton–Dickinson (BD, Becton–Dickinson, Germany) FACS Canto tm II flow cytometer and BD FACS Diva software. Indirect staining using just the secondary antibody was performed as negative standard, indicated in the figures as "negative." The data were acquired and analyzed as mean fluorescence intensity (MFI) using the FACS Diva software package (BD Biosciences). MFI values were compared with those observed in healthy untreated SGEC. This procedure was repeated for at least three passages.

Statistical analysis

Data were subjected to statistical analyses, calculating the mean percentage ± SE. Differences among groups were determined by *T* test using Excel 2007 software (Microsoft). Statistical significance was set at $*P < 0.05$ and $**P < 0.01$. All experiments were performed a minimum of three times.

Results

IL-17 enhanced TGF-β1 expression

We examined TGF-β1 expression to assess its role in EMT triggered by IL-17 in healthy SGEC (Fig. 1). To investigate whether or not IL-17 modulates TGF-β1 expression, healthy SGEC were cultured for 24 h in the presence of IL-17 (50 ng/mL). Total RNA was isolated, and gene expression was assessed by RT-PCR (Fig. 1a, b) and quantitative PCR (Fig. 1c). As seen, TGF-β1 mRNA expression increased significantly, up to threefold, with IL-17 treatment, thus reaching values similar to those found in pSS SGEC used as control ($p > 0.05$). To confirm whether or not the observed induction of TGF-β1 mRNA was correlated with the induction of TGF-β1 protein, healthy SGEC were cultured for 48 h in the presence of IL-17 (50 ng/mL), and TGF-β1 in conditioned medium collected from SGEC grown under IL-17 stimulation conditions was quantified by ELISA. TGF-β1 release is expressed as mean ± SE of three independent experiments and compared with that of untreated healthy SGEC. As shown in Fig. 1d, a representative ELISA of Il-17 treated healthy SGEC conditioned medium, TGF-β1 amounts were significantly increased as compared with untreated cells ($p < 0.01$). Furthermore, as shown in the Fig. 1e, f, western blot analysis confirmed the induction of TGF-β1 protein expression by IL-17 treatment.

Activation of the Erk signaling pathway was required for IL-17-TGF-β1-induced EMT in vitro

When stimulated with IL-17, healthy SGEC undergo EMT, a process characterized by the loss of E-cadherin from the plasma membrane, and cells acquire a spindle-like cell phenotype [16]. To extend our study, we sought to define the activation of the Erk1/2 pathway in normal SGEC under IL-17 stimulation conditions. RT-PCR analysis and Real-Time

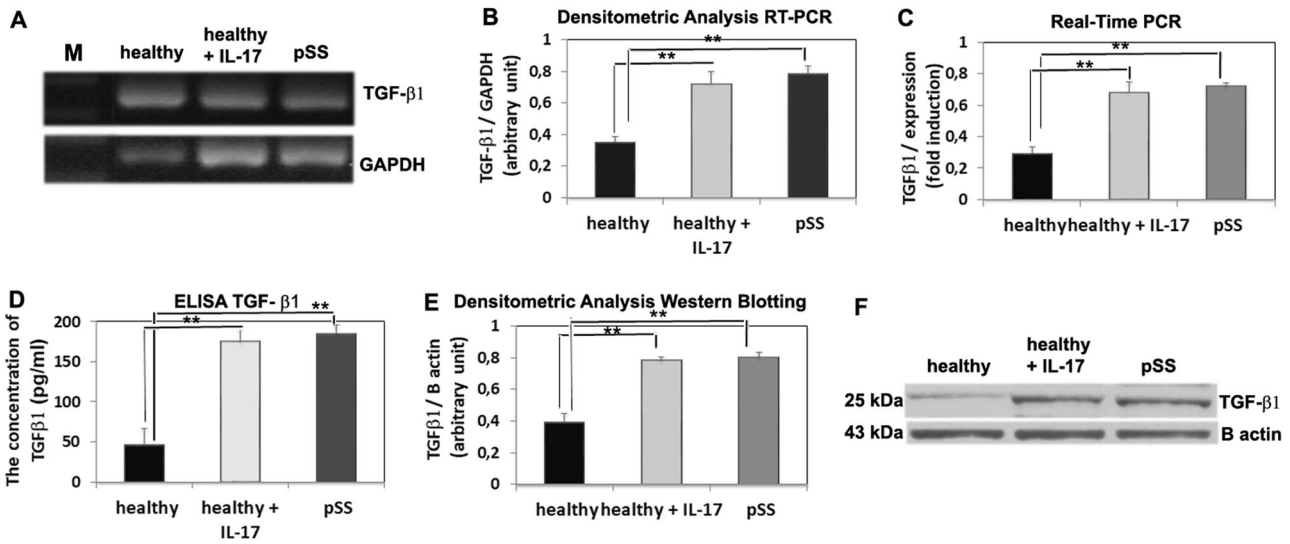

Fig. 1 IL-17 enhanced TGF-β1 expression. TGF-β1 gene and protein expression was quantified by semiquantitative RT-PCR (**a**), real-time PCR (**c**), western blotting (**f**), and ELISA (**d**) in in vitro cultured healthy SGEC treated with IL-17 for 24/48 h and in untreated control healthy SGEC. The images show that IL-17 treatment determined an increased TGF-β1 gene and protein expression. Band intensities were analyzed by densitometric analysis performed by gel image software, normalized against that of GAPDH for RT-PCR, and β-actin for western blotting, and expressed in arbitrary units (**b**, **e**). In all experimental procedures pSS SGEC were used as positive control. (Data represent mean ± SE; $n = 3$). Asterisks and arrowheads indicate statistical significance $p < 0.01$. M Marker.

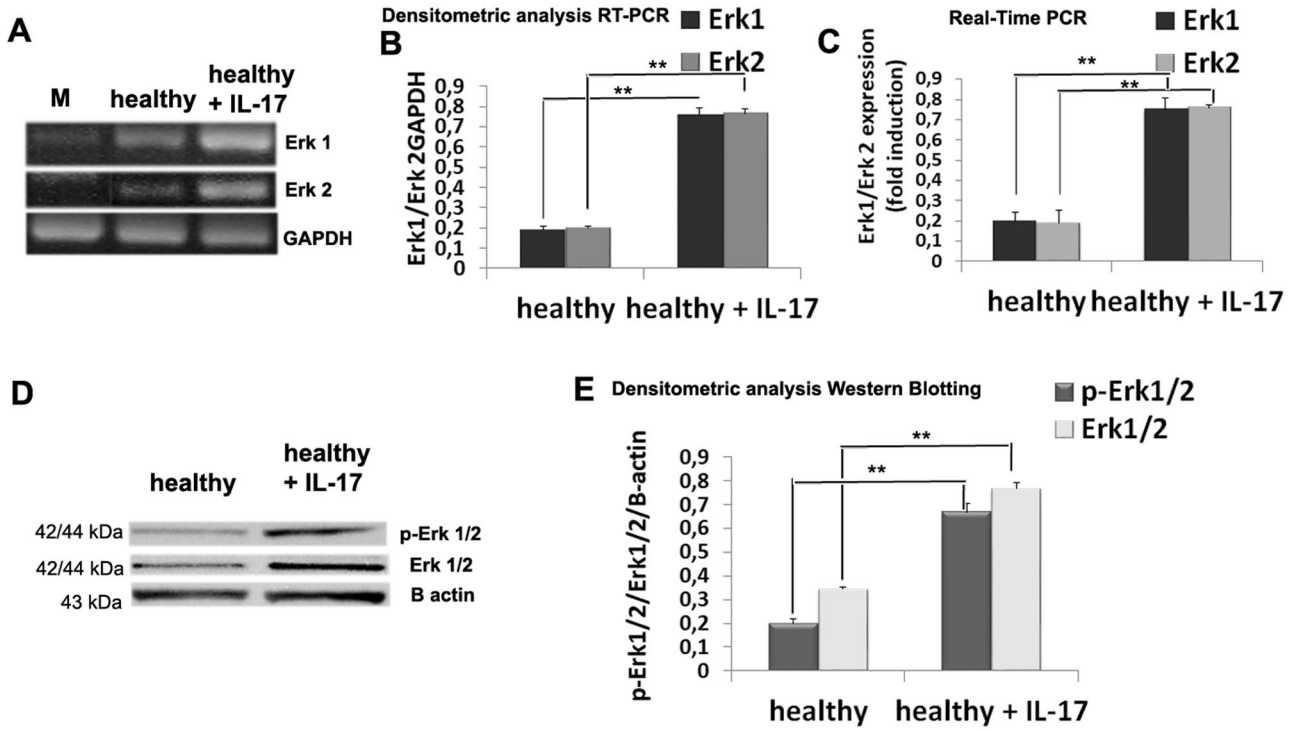

Fig. 2 IL-17 induced Erk1/2 gene and protein expression. Erk 1 and Erk 2 genes expression was quantified by semiquantitative RT-PCR (**a**, **b**) and real-time PCR (**c**) in in vitro cultured healthy SGEC treated for 24 h with IL-17 and in untreated control healthy SGEC. **d**, **e** Western blotting analysis of Erk 1/2 and phospho-Erk1/2 (p-Erk1/2) protein expression in in vitro cultured healthy SGEC treated for 48 h with IL-17 and in untreated control healthy SGEC. (Data represent mean ± SE; $n = 3$). Asterisks and arrowheads indicate statistical significance $p < 0.01$. M Marker.

PCR were performed on RNA from SGEC treated with IL-17 (Fig. 2a–c). The Erk1/2 gene exhibited a significantly increased expression (Fig. 2a–c), greater than twofold (Fig. 2c) ($p < 0.01$). Results from gene expression analyses suggested that in healthy SGEC, the Erk signaling pathway may be activated by IL-17. To study the protein expression level, total and phosphorylated Erk1/2 were determined using the cellular protein of healthy SGEC treated with 50 ng/mL of IL-17 for 48 h; western blot analysis revealed that IL-17 induced an increased expression of total Erk1/2, and the phosphorylation of Erk1/2 (Fig. 2d, e). To confirm the activation of Erk1/2 through phosphorylation in IL-17-treated healthy SGEC, we inhibited Erk1/2 activation by incubating IL-17-treated SGEC with a pharmacological agent that antagonizes the activity of MEKs, the upstream activators of Erk1 and Erk2. This MEK inhibitor, U0126, has been previously shown in numerous studies [26, 27] to effectively reduce the activity of MEK1 and MEK2. Figure 3 demonstrates the effects of the U0126 addition on the activation of Erk1/2 at both gene (Fig. 3a–c) and protein levels (Fig. 3d, e) in healthy SGEC treated by IL-17. demonstrating that the increased expression of total and active Erk1/2 following IL-17 treatment for 48 h was blocked by cotreatment with U0126, confirming the efficacy of this MEK inhibitor on IL-17-dependent activation of Erk1/2. Then we further investigated the relationship between the Erk pathway and TGFβ1 activation signaling mediated by IL-17 treatment. The role of Erk activation in TGF-β1-induced EMT is unclear. To test whether Erk signaling was necessary for IL-17-mediated-TGF-β1-induced EMT, Erk signaling was blocked using U0126, to explore the ability of MEK inhibition alone to promote epithelial characteristics in healthy SGEC. As shown in Fig. 4a, IL-17 induced EMT in healthy SGEC after 48 h of IL-17 treatment. In fact, in the absence of treatment (Fig. 4a), SGEC had an epithelial-like morphology, but upon IL-17 treatment, phase contrast microscopy revealed that the cells underwent a morphologic change from a cobblestone-like cell morphology to an elongated morphology (Fig. 4b). When healthy SGEC were treated with IL-17 in combination with the MEK1/2 inhibitor U0126 (IL-7 + U0126, Fig. 4c), the morphologic change induced by IL-17 alone was significantly blocked. Healthy SGEC were cultured in the presence of IL-17 with or without U0126 for 2 days (Fig. 4). In response to IL-17, TGF-β1 gene expression increased, E-cadherin gene expression decreased, and vimentin gene expression increased in SGEC (Fig. 4b–d) and confirming previous observations, U0126 cotreatment inhibited changes in TGF-β1, E-cadherin, and vimentin genes. The same trends were found in healthy SGEC, analyzing TGF-β1,

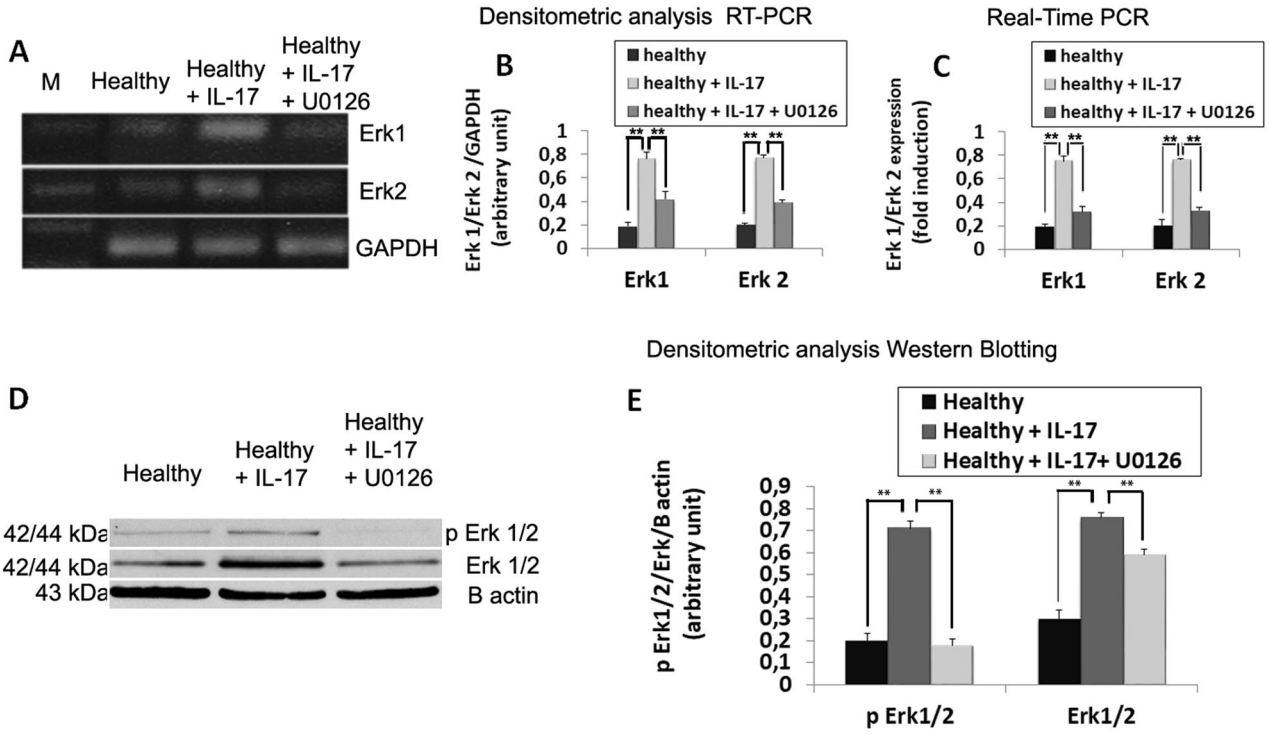

Fig. 3 U0126 inhibitor blocks noncanonical Erk kinase activity induced by IL-17. The effect of Erk inhibitor U0126 on Erk 1 and Erk 2 genes expression was quantified by semiquantitative RT-PCR (**a**, **b**) and real-time PCR (**c**) in untreated healthy SGEC, in healthy SGEC treated for 24 h with IL-17, and in SGEC treated with IL-17 plus U0126. **d**, **e** Western blotting analysis of Erk 1/2 and p-Erk1/2 protein expression in cultured healthy SGEC treated for 48 h with IL-17 and in SGEC treated with IL-17 + U0126; untreated healthy SGEC were used as control. As expected, cotreatment with IL-17 plus U0126 blocks the activation of Erk1/2. Bands intensities were analyzed by densitometric analysis performed by gel image software, normalized against that of GAPDH for RT-PCR (**b**) and β-actin for western blotting, and expressed in arbitrary units (**e**). (Data represent mean ± SE; $n = 3$). Asterisks and arrowheads indicate statistical significance $p < 0.01$. M Marker.

E-cadherin, and vimentin protein expression by western blot and flow cytometry (Fig. 4e–g), demonstrating the efficacy of U0126 in restoring the levels of TGF-β1, E-cadherin, and vimentin proteins in SGEC treated with IL-17.

IL-17 regulates TGF-β1/activity signaling by modulating Smad2/3 activity via phosphorylation

Previous studies of the relationship between IL-17 and TGF-β1 have not provided a definitive mechanistic link between the mediators; in addition, TGF-β1 mediated activation of the TGF-β1 receptor complex initiates signal transduction through the Smad2/3 pathway [28, 29]. Starting from these assumptions and considering that Sisto et al. have recently demonstrated that TGF-β1 is known to activate Smad2 and Smad3 in human healthy SGEC [16], we first evaluated the gene expression and activation status of Smad2/3 after 24 h of IL-17 treatment conditions. A comparison between the relative gene expression levels of Smad2/3 using RNA isolated from untreated and IL-17-24 h-treated healthy SGEC was performed (Fig. 5a–c); in the tested samples, we found that Smad2/3 gene expression significantly increased, more than twice (Fig. 5a, b, $p <$ 0.01) in comparison to the level observed in untreated SGEC (Fig. 5c, $p < 0.01$). In addition, healthy SGEC were stimulated for 48 h with or without IL-17 and, as shown in Fig. 5d, e, the expression of total Smad 2/3 and the phosphorylation of Smad2/3 at serine 423/425 was evaluated by western blot. An increased expression of total Smad 2/3 and a robust phosphorylation of Smad2/3 was observed in healthy SGEC stimulated with IL-17. We validated our results by flowcytometry (Fig. 5f) and observed an increased total Smad 2/3 expression and the phosphorylation and total protein of Smad2/3 in healthy SGEC following IL-17 exposure. Interestingly, increased Smad 2/3 gene and total protein expression and phospho-Smad2/3 protein levels after IL-17 treatment were not blocked by U0126, indicating that U0126 did not inhibit IL-17-mediated-TGF-β1 signaling activation through a direct effect on Smads (Fig. 5a–f).

Smad inhibition prevents IL-17 induction of TGF-β1-dependent EMT in healthy SGEC

In order to clearly determine which of the two main pathways, the Smad-dependent pathway or the MAPK/Erk1/2

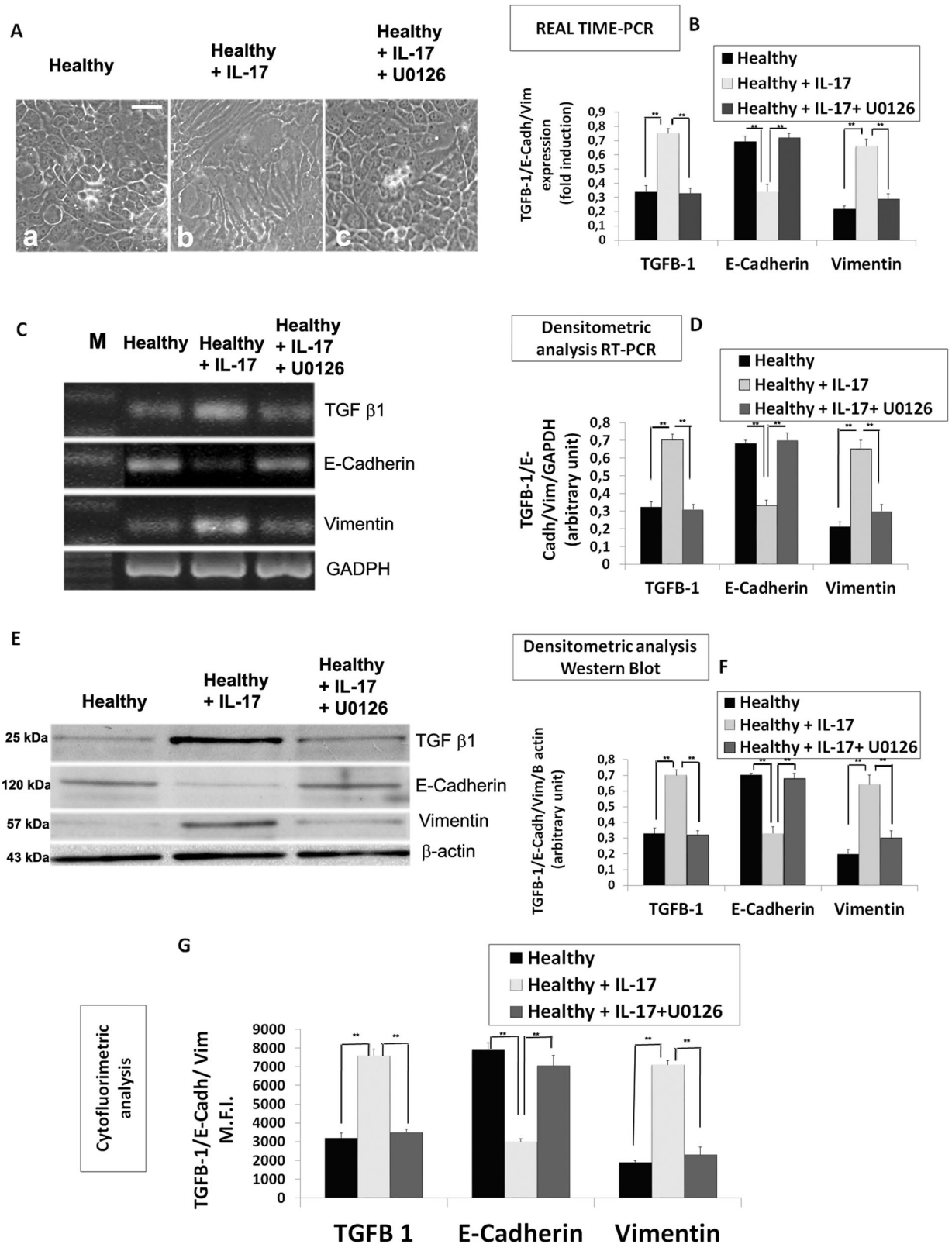

pathway, both of which can be activated by TGF-β1, was involved in IL-17-mediated EMT in SGEC, we firstly evaluated the efficacy of the pharmacological inhibitor of the Smad pathway, SB431542, in our experimental model. SB431542 is a potent and specific inhibitor of the TGF superfamily type I activin receptor-like kinase (ALK)

◀ **Fig. 4 The block of Erk1/2 signaling inhibited IL-17-dependent EMT in SGEC. a** Morphological changes detected in cultured SGEC treated with and without IL-17 and IL-17 plus U0126 Erk inhibitor for 48 h. Untreated SGEC (**a**); IL-17 treated cells (**b**); treatment of SGEC with IL-17 plus U0126 (**c**). Changes in cell morphology were assessed under phase contrast light microscopy (original magnification, ×20). Bar = 20 μm. TGF-β1, E-cadherin and vimentin genes expression was quantified by semiquantitative RT-PCR (**c**, **d**) and real-time PCR (**b**) in in vitro cultured healthy SGEC treated for 24 h with IL-17 and with IL-17 + U0126; untreated healthy SGEC were used as control. Band intensities were analyzed by densitometric analysis performed by gel image software, normalized against that of GAPDH and expressed in arbitrary units (**d**). (Data represent mean ± SE; $n = 3$). Asterisks and arrowheads indicate statistical significance $p < 0.01$. M Marker. **e** Western blot analysis of TGF-β1, E-cadherin, and vimentin in cultured untreated SGEC, and in healthy SGEC treated with IL-17 and IL-17 + U0126 for 48 h. Protein expressions were quantified using ImageJ software (**f**). The data are normalized to β-actin expression. Values are considered statistically significant at $*p < 0.05$ or $**p < 0.01$. All western blots were repeated a minimum of three times. **g** Summary of flow cytometry analysis for TGF-β1, E-cadherin, and vimentin SGEC expression in the presence of IL-17 and IL-17 + U0126. The mean fluorescence intensity (MFI) is shown. Data summarize three independent experiments (mean ± SE).

receptors ALK4, ALK5, and ALK7, which are responsible for the phosphorylation of Smad2/3 [30]. SB431542 was added to healthy SGEC treated with IL-17 to demonstrate the efficacious inhibition of total Smad 2/3 expression and Smad2/3 phosphorylation and activation. As shown in Fig. 6a–c, SB431542 was able to determine a significantly decreased Smad2 and Smad3 gene expression in comparison with IL-17 treated healthy SGEC ($p < 0.01$). A similar result was obtained when considering total and phospho-Smad2/3 protein expression (Fig. 6d–f). In fact, IL-17 + SB431542-treated healthy SGEC showed a lower Smad2/3 phosphorylation, comparable to untreated control cells, due to the blockade of IL-17-TGF-β-induced phosphorylation and activation of Smad2/3. Morphological evaluation of the effect of SB431542 addition to IL-17-treated healthy SGEC (Fig. 6d) revealed a clear attenuation of the IL-17-TGF-β-induced EMT in healthy SGEC, characterized by blockade of the cell morphology transformation from a cuboidal to an elongated spindle-like shape. These results further confirmed the efficacy of SB431542 in the system used to study IL-17-dependent EMT. Therefore, as shown in Fig. 6,

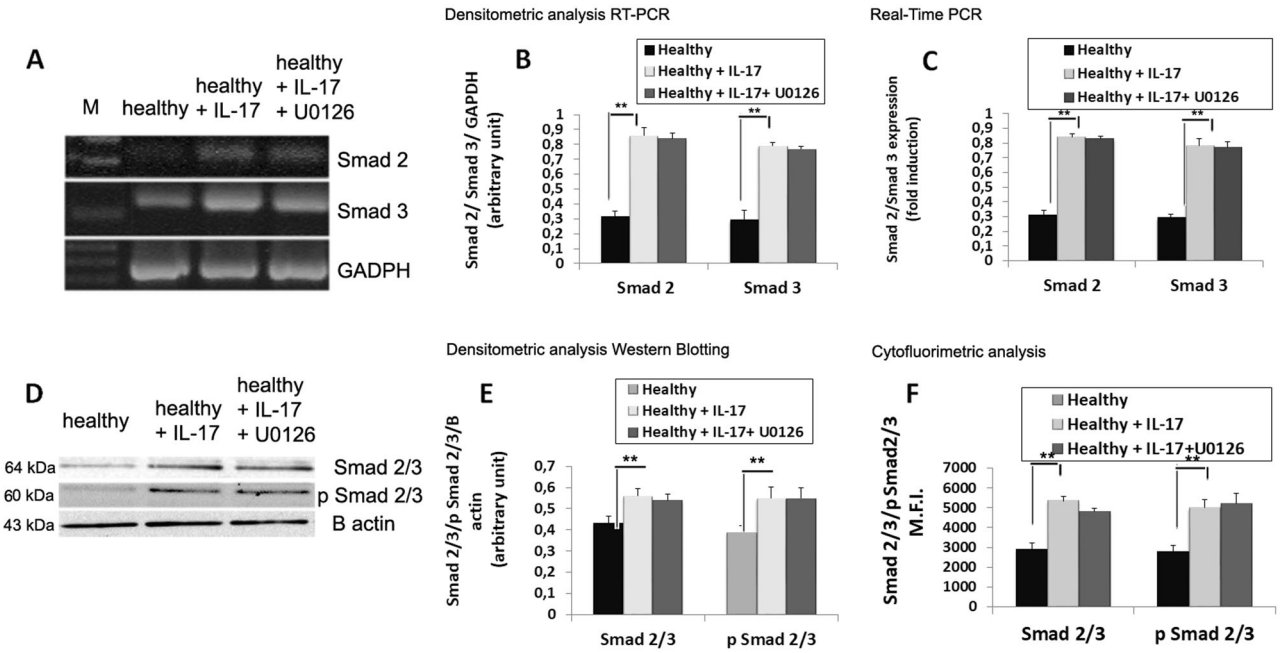

Fig. 5 Effect of Erk1/2 inhibitor U0126 on the Smad2/3 signaling pathway. Smad2 and Smad3 genes expression were quantified by semiquantitative RT-PCR (**a**, **b**) and real-time PCR (**c**) in in vitro cultured healthy SGEC treated for 24 h with or without IL-17 in the presence of the Erk inhibitor U0126. **d**, **e** Western blotting analysis of Smad2/3 and p-Smad 2/3 protein expression in in vitro cultured healthy SGEC treated for 24 h with or without IL-17 in the presence of the Erk inhibitor U0126. The treatment with IL-17 induced an increased Smad2/3 gene expression and Smad2/3 protein activation through phosphorylation. This increase was not blocked by U0126, indicating that U0126 did not inhibit IL-17-mediated-TGF-β1 signaling activation through a direct effect on Smads. Bands intensities were analyzed by densitometric analysis performed by gel image software, normalized against that of GAPDH for RT-PCR (**b**) and β-actin for western blotting, and expressed in arbitrary units (**e**). These results were confirmed by flow cytometry (**f**). (Data represent mean ± SE; $n = 3$). Asterisks and arrowheads indicate statistical significance ($**p < 0.01$). M Marker.

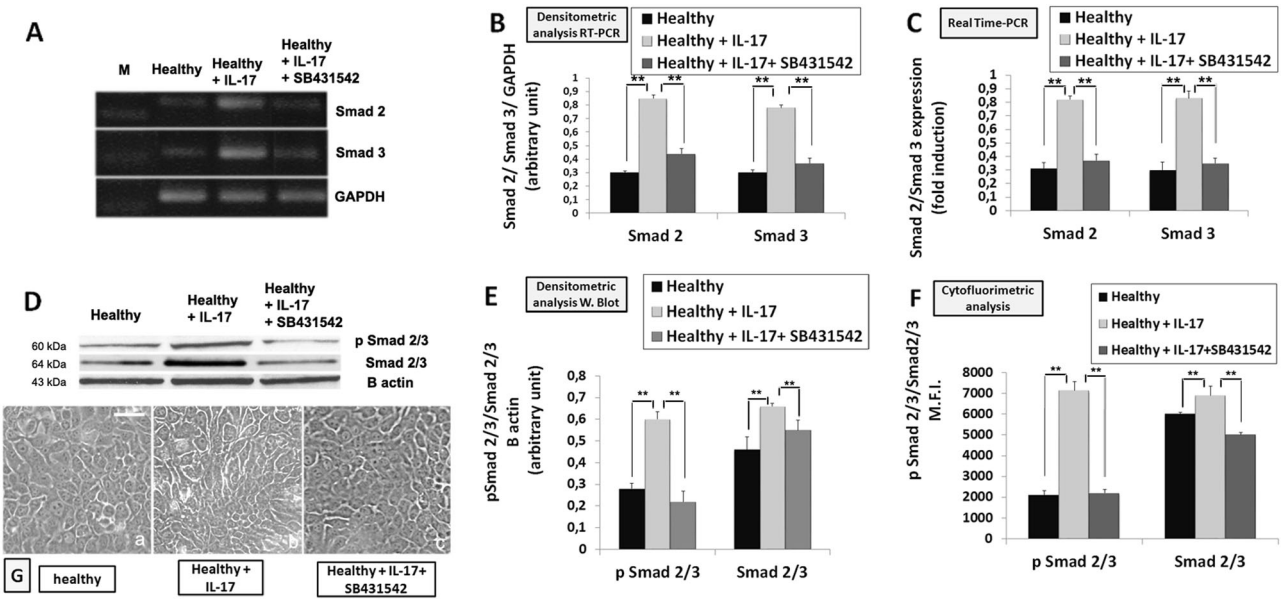

Fig. 6 Smad inhibitor SB431542 blocks canonical Smad activity induced by IL-17. The effect of Smad inhibitor SB431542 on Smad2 and Smad3 genes expression was quantified by semiquantitative RT-PCR (**a**, **b**) and real-time PCR (**c**) in untreated cultured healthy SGEC, in healthy SGEC treated for 24 h with IL-17 and in cells treated with IL-17 plus SB431542 Smad inhibitor. **d**, **e** Western blotting analysis of Smad 2/3 and p-Smad2/3 protein expressions in the SGEC treated for 48 h with IL-17, in SGEC treated with IL-17 + SB431542 and in untreated healthy SGEC as control. **f** Flow cytometry analysis for Smad2/3 and p-Smad2/3 expressions in the presence of IL-17 and IL-17 + SB431542. The mean fluorescence intensity (MFI) is shown. Cotreatment with IL-17 plus SB431542 inhibitor blocks the activation of the canonical Smad signaling pathway. **g** Represents morphological analysis changes detected in cultured SGEC treated with and without IL-17 and IL-17 plus SB431542 inhibitor. Untreated SGEC (**a**) show a clear pebble-like shape and cell–cell adhesion. IL-17-treated cells (**b**) show a decrease in cell–cell contacts and a more elongated morphological shape approaching a mesenchymal phenotype; while the treatment of SGEC with IL-17 plus Smad inhibitor (**c**) blocks the corresponsione morphological changes. Changes in cell morphology were assessed under phase contrast light microscopy (original magnification, ×20). Bar = 20 µm. Bands intensities were analyzed by densitometric analysis performed by gel image software, normalized against that of GAPDH for RT-PCR (**b**) and β actin for western blotting, and expressed as arbitrary units (**e**). (Data represent mean ± SE; $n = 3$). Asterisks and arrowheads indicate statistical significance (**$p < 0.01$). M Marker.

pretreatment with SB431542 significantly inhibited the enhancement of IL-17 dependent transcription of TGF-β1 gene and protein expression. In fact, as illustrated in Fig. 7a–c, TGF-β1 gene expression in IL-17-treated healthy SGEC resulted higher than the level observed following the addition of SB431542 ($p < 0.01$). At the protein level the same result was observed, showing a clear and significant reduction of TGF-β1 release following the addition of the inhibitor (Fig. 7d–g). Furthermore, as shown in Fig. 7a–g, SGEC treated with SB431542 together with IL-17 undergo upregulation of the E-cadherin gene and downregulation of vimentin gene expression compared with SGEC treated with IL-17 only ($p < 0.01$). We found the same results when analyzing E-cadherin and vimentin protein expression.

In the last step, as illustrated in Fig. 7h–j, in order to elucidate the role of the canonical Smad-mediated and noncanonical Erk-mediated signaling pathways in IL-17-TGF-β1-initiated EMT, we analysed Erk1/2 pathways activation in the presence of the pharmacological inhibitor SB431542 in healthy SGEC treated with IL-17. As shown, blocking Smad2/3 signaling with SB431542 did not affect basal or IL-17-TGF-β1-stimulated phosphorylation of Erk1/2, indicating that the canonical Smad-mediated and noncanonical Erk-mediated signaling pathways are mutually independent. Together, these results demonstrate that both the Smad2/3 and ERK pathways are responsible for IL-17-TGF-β1-induced EMT. Based on our findings, a possible scheme for TGF-β1-Smad2/3 and -ERK1/2 pathways activation by IL-17 is proposed in Fig. 8.

Discussion

A growing number of studies has indicated that the development of SG fibrosis in pSS could be attributed to EMT of SGEC in response to a variety of cytokines, typically TGF-β1 [31]. In the last years several experimental conditions have revealed the dichotomous nature of TGF-β during tumorigenesis, known as the "TGF-β Paradox," based on the demonstration that TGF-β acts as a potent anticancer agent, inhibiting the uncontrolled proliferation of various benign cell types and also acting during early-stage cancers, but then it promotes progression in cancer cells at later

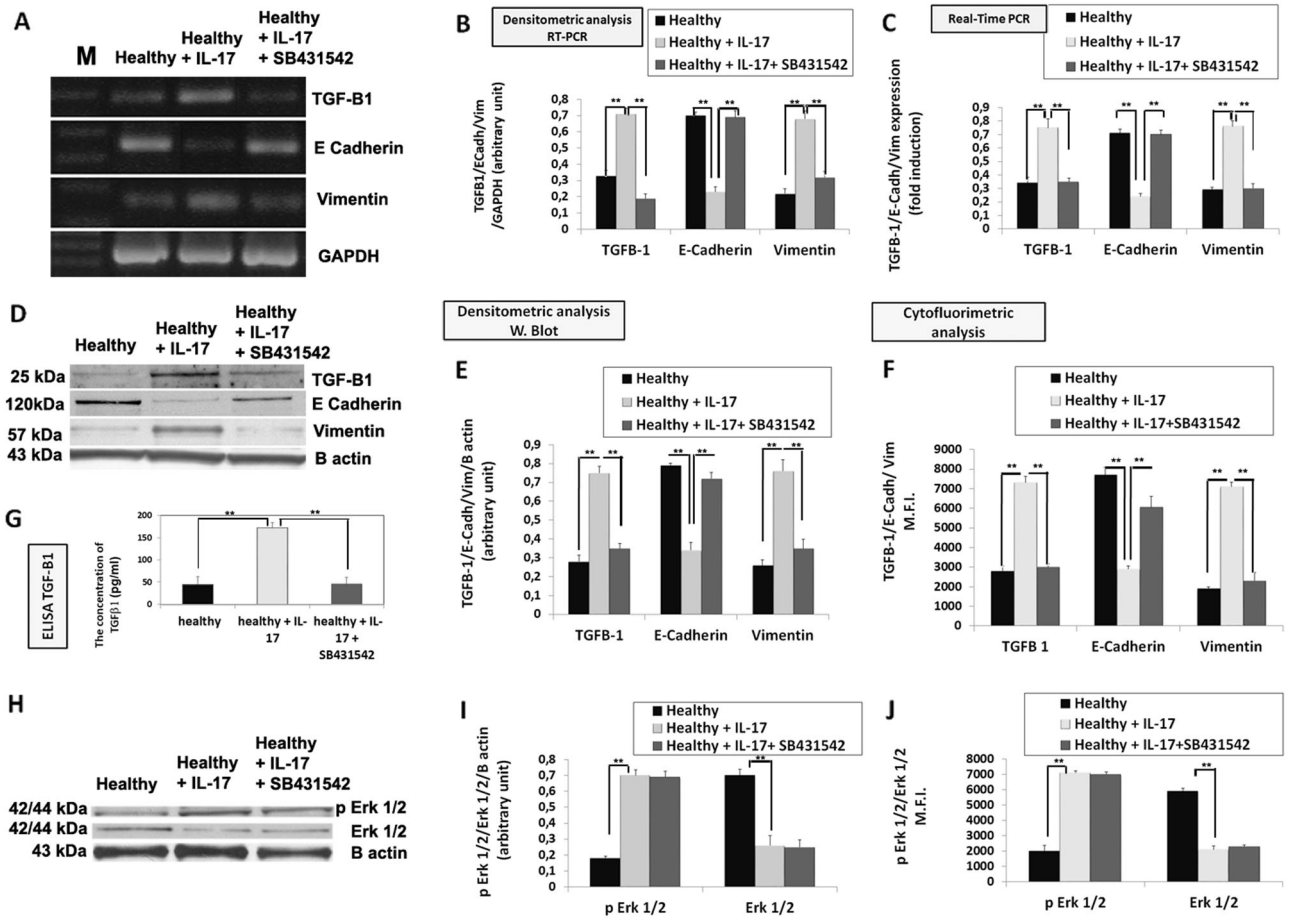

Fig. 7 Effects of Smad inhibitor SB431542 on IL-17-dependent activation of EMT. The effect of Smad inhibitor SB431542 on TGF-β1, E-cadherin and vimentin genes expression was quantified by semiquantitative RT-PCR (**a**, **b**) and real-time PCR (**c**) in untreated cultured healthy SGEC, in healthy SGEC treated for 24 h with IL-17 and in cells treated with IL-17 plus SB431542 Smad inhibitor. Bands intensities were analyzed by densitometric analysis performed by gel image software, normalized against that of GAPDH and expressed in arbitrary units (**b**). **d**–**f** Western blotting and flow cytometry analysis of TGF-β1, E-cadherin, and vimentin protein expression in cultured healthy SGEC treated for 48 h with IL-17 or IL-17 + SB431542 and in untreated healthy SGEC. Protein expression changes observed by western blotting and flow cytometric analysis are in agreement with the results monitored by semiquantitative RT-PCR and real-time PCR analysis. The mean fluorescence intensity (MFI) is shown for flow cytometry. Proteins expressions were quantified using ImageJ software (**e**). **g** For TGF-β1 protein expression ELISA was also performed on the culture medium of SGEC treated with or without IL-17 for 48 h in the presence or not of the Smad2/3 inhibitor SB431542, confirming results obtained with the other experimental procedures. **h**–**j** The effect of Smad inhibitor SB431542 on p-Erk1/2 expression in SGEC treated with IL-17 and analyzed by western blotting (**h**, **i**) and flow cytometry (**j**). Values are considered statistically significant at $*p < 0.05$ or $**p < 0.01$. (Data represent mean ± SE; $n = 3$).

stages [32]. The TGF-β Paradox manifestations are closely related to the initiation of EMT in the development and progression of malignancies. The pathological reactivation of EMT through the canonical TGF-β1-dependent Smad 2/3 pathway plays a critical role in carcinogenesis, promoting cancer invasion and metastasis, but also in various chronic fibrotic diseases, including pSS [15, 16, 33]. In this study, we investigated the role of IL-17 in the activation of the canonical TGF-β1/Smad pathway, focusing on the interaction of Smad 2/3 signaling with the noncanonical Erk1/2 pathway in TGFβ1-induced EMT in human SGEC. We found that the activation of Erk 1/2 signaling by TGF-β1, in healthy SGEC treated with IL-17, is independent of canonical IL-17-dependent TGFβ1/Smad signaling, because blocking Smad2/3 signaling with the specific inhibitor SB431542 did not affect the basal or IL-17-TGF-β1-stimulated phosphorylation of Erk1/2, indicating that both the canonical Smad2/3 and noncanonical Erk 1/2 pathways are responsible for IL-17- TGF-β1-induced EMT.

These observations provide compelling evidence further supporting our emerging view that IL-17 is an important factor promoting EMT in pathological organ fibrosis settings during chronic inflammatory diseases. Increasing evidence has suggested that IL-17 is clearly linked to EMT in lung inflammatory diseases [34] and pulmonary fibrosis [34, 35]. In obliterative bronchiolitis, IL-17-mediated EMT-dependent type V collagen deposition via TGF-β1-dependent signaling was shown [35], and recently the inhibitory

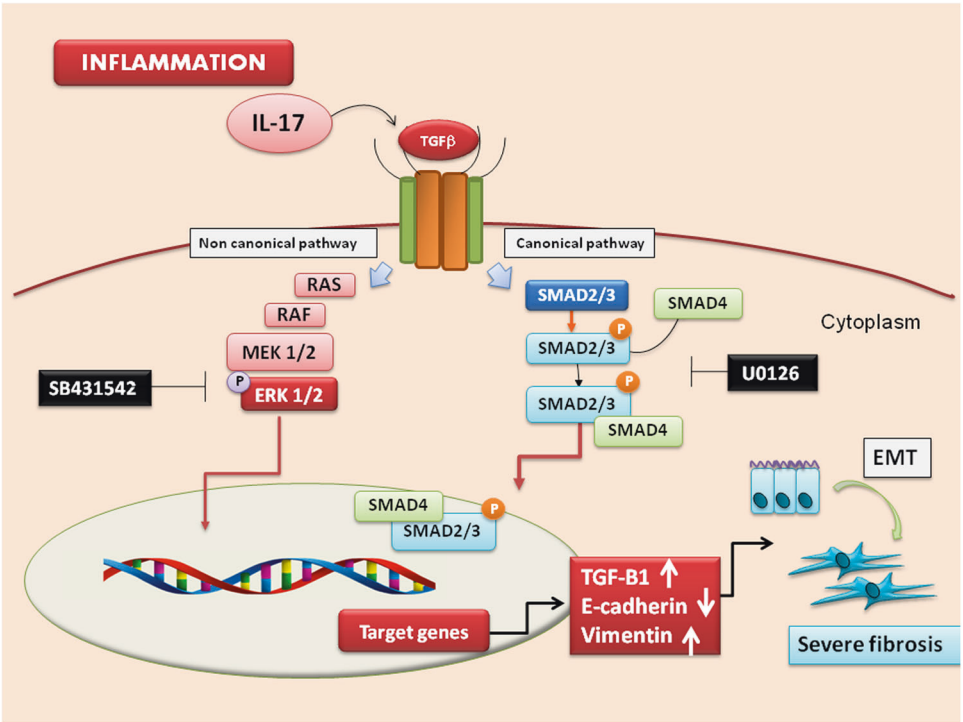

Fig. 8 Postulated mechanism of IL-17-TGF-β1-induced EMT in healthy SGEC. TGF-β1 signals through both the canonical Smad2/3 pathway and the noncanonical Erk1/2 pathway. The canonical pathway requires the phosphorylation of Smad2/3, and can be blocked by SB431542. The noncanonical pathway requires the phosphorylation of Erk1/2, and can be inhibited by U0126 but not through the addition of SB431542. TGF-β1 activates both the canonical and noncanonical pathways triggering the IL-17-dependent EMT in healthy SGEC.

action of an IL-17 antagonist on chronic inflammatory responses and pulmonary fibrosis, acting in a TGF-β1-dependent manner, was demonstrated [34]. In addition, IL-17 expression is widely recognized as a potential key factor in the progression of fibrosis in several major organs such as the heart [36], kidney [37], and liver [38]. In the last year, this has been shown also in SGs, where IL-17 determines gene and protein expression changes of the EMT markers E-cadherin, vimentin, and collagen type I in healthy SGEC, leading to morphological alterations typical of transdifferentiation toward a mesenchymal cell type similar to that observed in pSS SGEC [15, 16].

TGF-β1 is proposed as the most prominent inflammatory inducer of pathological fibrosis in the kidney [39–41], lung [42], and liver [43]. In fact, TGF-β1 overproduction promotes evident fibrotic changes affecting physiological organ function [44–46]. In addition, a recent study implicated TGF-β1 as a mediator of fibrosis observed in pSS, since increased TGF-β1 levels were detected in pSS SGs tissues. This phenomenon seems to be associated with chronic inflammatory conditions, determining an excessive fibrotic tissue deposition in pSS SGs [15]. These studies confirmed that a cascade of events is activated in pSS SGs, that determines changes in the expression of TGF-β1-dependent factors, Smads, Snail, and the activation of a profibrotic transcriptional program [14, 15]. However, the exact mechanism involved in cytokines-dependent TGF-β1-related EMT activation in the pathogenesis of pSS remains less well documented.

For our study purposes, firstly human SGEC derived from healthy subjects were cultured in the presence of IL-17 as a model to simulate pSS, and the effect on the TGF-β1 gene and protein expression was investigated, demonstrating that IL-17 treatment can change TGF-β1 expression in healthy SGEC. This result was in accordance with data obtained by Meng et al. [38, 40] who found that IL-17 signaling facilitates the production of IL-6, IL-1β, and TNF-α by inflammatory cells, and increases the expression of TGF-β1, the major profibrogenic cytokine. Furthermore, Okamoto et al. [47] demonstrated that the addition of recombinant IL-17 to a skin fibroblast cell line culture determines increased TGF-β1, connective tissue growth factor, and collagen production. Known important intracellular factors of the TGF-β1 signaling pathway are members of the Smad family, which have crucial key roles in promoting TGF-β-induced EMT. TGF-β isoforms exert their cellular effects by binding to the TGF-β type II receptor (TβRII), and this binding facilitates the activation of TGF-β type I receptor (TβRI) kinase, which leads to the activation of Smad2 and Smad3. Phosphorylated Smads partner with cytosolic Smad4 and form a heteromeric Smad complex, which translocates to the nucleus and cooperates with other transcription factors, coactivators, and corepressors to regulate the transcription of specific genes [48, 49]. Sisto et al. [15, 16] found that TGF-β1 induces EMT via the TGF-β1/SMAD/Snail signaling pathway in healthy SGEC. Given the role of the Smad signaling pathway in TGF-β family signaling, as a second step we

investigated whether IL-17 may induce EMT through the TGF-β/Smad signaling pathway. To address this issue, we conducted studies with healthy SGEC to assess the impact of phosphorylated Smad2/3 and total Smad2/3 expression during IL-17-stimulated EMT. We found that IL-17 treatment significantly increased the phosphorylation of Smad2/3 in healthy SGEC. This suggested that the Smad2/3 pathway is involved in EMT stimulated by IL-17. To further elucidate the role of the Smad pathway in IL-17-stimulated EMT, SB431542, a potent and specific inhibitor of TβRI kinases (ALK-4, −5, −7), was used to inhibit IL-17-induced phosphorylation of Smad2/3 in healthy SGEC. We found that treatment of SGEC with SB431542 can inhibit morphological changes and phenotypic markers expression, such as downregulated E-cadherin expression and upregulated vimentin expression.

In addition, TGF-β1 can also activate non-Smad signaling pathways [50, 51], such as the MAPK signaling cascade including Erk1/2. In addition, the Erk1/2 signaling pathway has a complex and crucial correlation with the TGF-β1 system in controlling carcinogenesis [52] and inflammation [53]. Likewise, Erk1/2 activity has been considered an essential condition for TGF-β1-mediated EMT [54]. In human lung biopsy samples an augmented Erk1/2 signaling was observed in idiopathic pulmonary fibrosis samples compared with normal control lungs [55]. Madala et al. [56] demonstrated that blocking the Mek/Erk pathway in vivo attenuated the progression of both fibrosis and physiologic alterations in the lung. Therefore, we also conducted studies to explore the role of the ERK pathway in IL-17-mediated EMT in healthy SGEC. Like Smad2/3, enhanced Erk phosphorylation can be consistently detected in healthy SGEC after IL-17 stimulation. Furthermore, treatment of healthy SGEC with U0126, an Erk1/2 inhibitor, inhibited the corresponding morphological changes and phenotypic markers expression in SGEC. Therefore, our data support the concept that IL-17 enhances Erk1/2 activity during the induction of EMT. Nevertheless, after inhibiting canonical TGFβ/Smad2/3 signaling transduction, no effect on the activation of Erk1/2 induced by IL-17 dependent TGFβ1 release was detected. These data indicate that IL-17-dependent TGFβ1-induced ERK1/2 activation is independent of the IL-17-dependent TGFβ1/Smad pathway in SGEC, providing evidence that TGF-β1-induced activation of Erk1/2 is independent of canonical TGFβ1/Smad signaling in pSS. These results do not only provide new insights into the cellular mechanisms that mediate EMT in pSS, but also offer potential for novel treatment targets that could benefit patients by reducing SG fibrosis and promoting improved glandular function.

Acknowledgements We are grateful to M.V.C. Pragnell, B.A., a professional scientific text editor, for critical reading of the paper.

Compliance with ethical standards

Conflict of interest The authors declare that they have no conflict of interest.

Publisher's note Springer Nature remains neutral with regard to jurisdictional claims in published maps and institutional affiliations.

References

1. Wynn TA. Cellular and molecular mechanisms of fibrosis. J Pathol. 2008;214:199–210.
2. López-Novoa JM, Nieto MA. Inflammation and EMT: an alliance towards organ fibrosis and cancer progression. EMBO Mol Med. 2009;1:303–14.
3. Borthwick LA, Wynn TA, Fisher AJ. Cytokine mediated tissue fibrosis. Biochim Biophys Acta. 2013;1832:1049–60.
4. Chen L, Deng H, Cui H, Fang J, Zuo Z, Deng J, et al. Inflammatory responses and inflammation-associated diseases in organs. Oncotarget. 2017;9:7204–18.
5. Radisky DC, Kenny PA, Bissell MJ. Fibrosis and cancer: do myofibroblasts come also from epithelial cells via EMT? J Cell Biochem. 2007;101:830–9.
6. Kalluri R, Weinberg RA. The basics of epithelial-mesenchymal transition. J Clin Investig. 2009;119:1420–28.
7. Nieto MA, Huang RY, Jackson RA, Thiery JP. EMT: 2016. Cell. 2016;166:21–45.
8. Aiello NM, Maddipati R, Norgard RJ, Balli D, Li J, Yuan S, et al. EMT subtype influences epithelial plasticity and mode of cell migration. Dev Cell. 2018;45:681–95.
9. Wynn TA, Ramalingam TR. Mechanisms of fibrosis: therapeutic translation for fibrotic disease. Nat Med. 2012;18:1028–40.
10. Wang Y, Hou Z, Qiu M, Ye Q. Risk factors for primary Sjögren syndrome-associated interstitial lung disease. J Thorac Dis. 2018;10:2108–17.
11. Moutsopoulos HM, Chused TM, Mann DL, Klippel JH, Fauci AS, Frank MM, et al. Sjogren's syndrome (Sicca syndrome): current issues. Ann Intern Med. 1980;92:212–26.
12. Humphreys-Beher MG, Peck AB. New concepts for the development of autoimmune exocrinopathy derived from studies with the NOD mouse model. Arch Oral Biol. 1999;44:S21–5.
13. Roescher N, Tak PP, Illei GG. Cytokines in Sjogren's syndrome: potential therapeutic targets. Ann Rheum Dis. 2010;69:945–8.
14. Wang T, Liu Y, Zou JF, Cheng ZS. Interleukin-17 induces human alveolar epithelial to mesenchymal cell transition via the TGF-β1 mediated Smad2/3 and ERK1/2 activation. PLoS ONE. 2017;12:e0183972.
15. Sisto M, Lorusso L, Ingravallo G, Tamma R, Ribatti D, Lisi S. The TGF-β1 signaling pathway as an attractive target in the fibrosis pathogenesis of Sjögren's syndrome. Mediat Inflamm. 2018;26:eCollection 2018.
16. Sisto M, Lorusso L, Tamma R, Ingravallo G, Ribatti D, Lisi S. Interleukin-17 and -22 synergy linking inflammation and EMT-dependent fibrosis in Sjögren's syndrome. Clin Exp Immunol. 2019;198:261–72.
17. Biernacka A, Dobaczewski M, Frangogiannis NG. TGF-β signaling in fibrosis. Growth Factors. 2011;29:196–202.
18. Zhang YE. Non-Smad pathways in TGF-beta signaling. Cell Res. 2009;19:128–39.
19. Yoshimura A, Wakabayashi Y, Mori T. Cellular and molecular basis for the regulation of inflammation by TGF-beta. J Biochem. 2010;147:781–92.

20. Kuwabara T, Ishikawa F, Kondo M, Kakiuchi V. The role of IL-17 and related cytokines in inflammatory autoimmune diseases. Mediat Inflamm. 2017;2017:3908061.
21. Zhang J, Wang D, Wang L, Wang S, Roden AC, Zhao H, et al. Profibrotic effect of IL-17A and elevated IL-17RA in idiopathic pulmonary fibrosis and rheumatoid arthritis-associated lung disease support a direct role for IL-17A/IL-17RA in human fibrotic interstitial lung disease. Am J Physiol Lung Cell Mol Physiol. 2019;316:L487–97.
22. Vitali C, Bombardieri S, Jonsson R, Moutsopoulos HM, Alexander EL, Carsons SE, European Study Group on Classification Criteria for Sjögren's Syndrome, et al. Classification criteria for Sjögren's syndrome: a revised version of the European criteria proposed by the American-European Consensus Group. Ann Rheum Dis. 2002;612:554–8.
23. Sens DA, Hintz DS, Rudisill MT, Sens MA, Spicer SS. Explant culture of human submandibular gland epithelial cells: evidence for ductal origin. Lab Investig. 1985;52:559–67.
24. Kapsogeorgou EK, Dimitriou ID, Abu-Helu RF, Moutsopoulos HM, Manoussakis MN. Activation of epithelial and myoepithelialcells in the salivary glands of patients with Sjögren's syndrome: high expression of intercellular adhesion molecule-1 (ICAM.1) in biopsys pecimens and cultured cells. Clin Exp Immunol. 2001;124:126–33.
25. Laping NJ, Grygielko E, Mathur A, Butter S, Bomberger J, Tweed C, et al. Inhibition of transforming growth factor (TGF)-beta1-induced extracellular matrix with a novel inhibitor of the TGF-beta type I receptor kinase activity: SB-431542. Mol Pharmacol. 2002;62:58–64.
26. Frémin C, Meloche S. From basic research to clinical development of MEK1/2 inhibitors for cancer therapy. J Hematol Oncol. 2010;3:8–15.
27. Wu PK, Park V. MEK1/2 inhibitors: molecular activity and resistance mechanisms. Semin Oncol. 2015;42:849–62.
28. Wrighton KH, Lin X, Feng XH. Phospho-control of TGF-beta superfamily signaling. Cell Res. 2009;19:8–20.
29. Schnaper HW, Hayashida T, Poncelet AC. It's a Smad world: regulation of TGF-beta signaling in the kidney. J Am Soc Nephrol. 2002;13:1126–8.
30. Inman GJ, Nicolas FJ, Callahan JF, Harling JD, Gaster LM, Reith AD, et al. SB431542 is a potent and specific inhibitor of transforming growth factor-beta superfamily type I activin receptor-likekinase (ALK) receptors ALK4, ALK5, and ALK7. Mol Pharmacol. 2002;62:65–74.
31. Wendt MK, Allington TM, Schiemann WP. Mechanisms of the epithelial-mesenchymal transition by TGF-beta. Future Oncol. 2009;5:1145–68.
32. Morrison CD, Parvani JG, Schiemann WP. The relevance of the TGF-β Paradox to EMT-MET programs. Cancer Lett. 2013;341:30–40.
33. Zhu Y, Gu J, Zhu T, Jin C, Hu X, Wang X. Crosstalk between Smad 2/3 and specific isoforms of ERK in TGF-β1-induced TIMP-3 expression in rat chondrocytes. J Cell Mol Med. 2017;21:1781–90.
34. Mi S, Li Z, Yang HZ, Liu H, Wang JP, Ma YG, et al. Blocking IL-17A promotes the resolution of pulmonary inflammation and fibrosis via TGF-β1-dependent and -independent mechanisms. J Immunol. 2011;187:3003–14.
35. Vittal R, Fan L, Greenspan DS, Mickler EA, Gopalakrishnan B, Gu H, et al. IL-17 induces type V collagen overexpression and EMT via TGF-β-dependent pathways in obliterative bronchiolitis. Am J Physiol Lung Cell Mol Physiol. 2013;304:L401–14.
36. Valente AJ, Yoshida T, Gardner JD, Somanna N, Delafontaine P, Chandrasekar B. Interleukin-17A stimulates cardiac fibroblast proliferation and migration via negative regulation of the dual-specificity phosphatase MKP-1/DUSP-1. J Cell Signal. 2012;24:560–8.
37. Liu L, Li FG, Yang M, Wang L, Chen Y, Wang L, et al. Effect of pro-inflammatory interleukin-17A on epithelial cell phenotype inversion in HK-2 cells in vitro. Eur Cytokine Netw. 2016;27:27–33.
38. Meng F, Wang K, Aoyama T, Grivennikov SI, Paik Y, Scholten D, et al. Interleukin-17 signaling in inflammatory, Kupffer cells, and hepatic stellate cells exacerbates liver fibrosis in mice. Gastroenterology. 2012;143:765–76.
39. Meng XM, Nikolic-Paterson DJ, Lan HY. Inflammatory processes in renal fibrosis. Nat Rev Nephrol. 2014;10:493–503.
40. Meng XM, Tang PM, Li J, Lan HY. TGF-β/Smad signaling in renal fibrosis. Front Physiol. 2015;6:82.
41. Meng XM, Nikolic-Paterson DJ, Lan HY. TGF-β: the master regulator of fibrosis. Nat Rev Nephrol. 2016;12:325–38.
42. Willis BC, Borok Z. TGF-β-induced EMT: mechanisms and implications for fibrotic lung disease. Am J Physiol Lung Cell Mol Physiol. 2007;293:L525–34.
43. Fabregat I, Moreno-Càceres J, Sánchez A, Dooley S, Dewidar B, Giannelli G, et al. IT-LIVER Consortium. TGF-β signaling and liver disease. FEBS J. 2016;283:2219–32.
44. Kanzler S, Lohse AW, Keil A, Henninger J, Dienes HP, Schirmacher P, et al. TGF-β1 in liver fibrosis: an inducible transgenic mouse model to study liver fibrogenesis. Am J Physiol. 1999;276:G1059–68.
45. Kaimori A, Potter J, Kaimori JY, Wang C, Mezey E, Koteish A. Transforming growth factor-beta1 induces an epithelial-to-mesenchymal transition state in mouse hepatocytes in vitro. J Biol Chem. 2007;282:22089–101.
46. Liu N, He S, Ma L, Ponnusamy M, Tang J, Tolbert E, et al. Blocking the class I histone deacetylase ameliorates renal fibrosis and inhibits renal fibroblast activation via modulating TGF-beta and EGFR signaling. PLoS ONE. 2013;8:e54001.
47. Okamoto Y, Hasegawa M, Matsushita T, Hamaguchi Y, Huu DL, Iwakura Y, et al. Potential roles of interleukin-17A in the development of skin fibrosis in mice. Arthritis Rheum. 2012;264:3726–35.
48. Moustakas A, Souchelnytskyi S, Heldin CH. Smad regulation in TGF-beta signal transduction. J Cell Sci. 2001;114:4359–69.
49. Zi Z, Chapnick DA, Liu X. Dynamics of TGF-β/Smad signaling. FEBS Lett. 2012;586:1921–8.
50. Moustakas AC, Heldin H. Non-Smad TGF-beta signals. J Cell Sci. 2005;118:3573–84.
51. Zhang YE. Non-Smad signaling pathways of the TGF-β family. Cold Spring Harb Perspect Biol. 2017;9:a02212.
52. Wakefield LM, Roberts AB. TGF-beta signaling: positive and negative effects on tumorigenesis. Curr Opin Genet Dev. 2002;12:22–9.
53. Zhao M, Mishra L, Deng CX. The role of TGF-β/SMAD4 signaling in cancer. Int J Biol Sci. 2018;14:111–23.
54. Xie L, Law BK, Chytil AM, Brown KA, Aakre ME, Moses HL. Activation of the Erk pathway is required for TGF-beta1-induced EMT in vitro. Neoplasia. 2004;6:603–10.
55. Antoniou KM, Margaritopoulos GA, Soufla G, Symvoulakis E, Vassalou E, Lymbouridou R, et al. Expression analysis of Akt and MAPK signaling pathways in lung tissue of patients with idiopathic pulmonary fibrosis (IPF). J Recept Signal Transduct Res. 2010;30:262–9.
56. Madala SK, Schmidt S, Davidson C, Ikegami M, Wert S, Hardie WD. MEK-ERK pathway modulation ameliorates pulmonary fibrosis associated with epidermal growth factor receptor activation. Am J Respir Cell Mol Biol. 2012;46:380–8.